Spectroscopic ellipsometry of Ni3Al in comparison with band-structure calculations

Heide, P.A.M. van der; Buiting, J.J.M.; Dam, L.M. ten; Schreurs, L.W.M.; Groot, R.A. de; Vroomen, A.R. de

Published in:
Journal of Physics F%3A Metal Physics

DOI:
10.1088/0305-4608/15/5/024

J. Phys. F: Met. Phys. **15** (1985) 1195–1201. Printed in Great Britain

Spectroscopic ellipsometry of Ni_3Al in comparison with band-structure calculations

P A M van der Heide, J J M Buiting, L M ten Dam, L W M Schreurs, R A de Groot and A R de Vroomen

Research Institute for Materials, Faculty of Sciences, University of Nijmegen, Toernooiveld, 6525 ED Nijmegen, The Netherlands

Received 8 October 1984, in final form 23 November 1984

Abstract. The optical constants of Ni_3Al from 0.5 to 5.3 eV have been determined by means of spectroscopic ellipsometry at room temperature under ultra-high vacuum conditions. Measurements were performed on a single crystal and a polycrystalline sample, which gave identical results. The results are compared with optical properties calculated from the band-structure calculation by Buiting *et al*. The experimental results are in good agreement with the predictions from the band-structure calculation.

1. Introduction

There is still considerable debate about the nature of magnetic phase transitions in metallic compounds, such as the transition from exchange-enhanced paramagnetism to weak ferromagnetism in Ni_3Al. The weak itinerant ferromagnet Ni_3Al has received quite a lot of attention over the last fifteen years because of its low T_c of 40 K. Various types of experiment have been performed on Ni_3Al, for example measurements of magnetic properties (de Boer 1969, Buis 1979), low-temperature specific heat (de Dood and de Châtel 1973) and neutron scattering (Bernhoeft *et al* 1983). Several band-structure calculations have been performed (Fletcher 1972, Hackenbracht and Kübler 1980, Buiting *et al* 1983). The reliability of these band structures was tested by de Haas–van Alphen measurements (Lonzarich *et al* 1982), which give information about electrons at E_F.

Angle-integrated XPS measurements were performed by Fuggle *et al* (1983), which gave the density of states below E_F. Their measurements showed that the XPS valence-band spectra of Ni_3Al are dominated by peaks from nickel d bands, which are shifted roughly 0.5 eV away from E_F with respect to nickel.

Optical studies such as spectroscopic ellipsometry give information about intraband and interband transitions, which can be compared directly with theoretical results calculated from band structures to give information about states several eV below E_F. The skin depth in most materials for light in the range 0.5–6.0 eV varies from several thousand to several hundred ångströms. These measurements are less sensitive to surface effects than are photoemission experiments, which is a considerable advantage for the study of compounds whose surfaces are not easily obtained in a stoichiometric and clean condition.

0305-4608/85/051195 + 07$02.25

2. Experiment

The equipment used for measuring the optical properties consists of a photometric ellipsometer, which under ultra-high vacuum conditions gives best results in the range 0.5–5.6 eV.

This ellipsometer has been described elsewhere (see, e.g., van der Heide *et al* 1984). Linearly polarised light is incident on the sample at an angle of 70°. The resulting intensities of the light reflected by the sample are measured at discrete positions of a rotatable analyser.

From these data the ellipsometric parameters $\tan\psi$ and $\cos\Delta$ (Beattie 1955) can be calculated and they enable us to determine the dielectric constants ε_1 and ε_2. Because Ni_3Al has a cubic crystal structure (FCC, Cu_3Au structure) the dielectric constants can be calculated using the formulae for isotropic materials (Born and Wolf 1959). To compare the measurements with band-structure calculations we also derived the joint density of states (JDOS) and the optical conductivity, in which effects of the band structure are most clearly pronounced.

The relation between ε_2 and these two quantities is given by

$$\text{JDOS} = A \sum_{\text{i,f}} \int \mathrm{d}\boldsymbol{k}\, \delta(E_\text{f}(\boldsymbol{k}) - E_\text{i}(\boldsymbol{k}) - \hbar\omega) = \omega^2 \varepsilon_2 \tag{1}$$

$$\sigma = \omega\varepsilon_2 \tag{2}$$

where i and f denote initial and final states and $\hbar\omega$ is the photon energy used.

In the measurements energy spacings of 0.03 eV were used in the visible and ultraviolet parts of the spectrum and spacings of 0.01 eV in the infrared.

Measurements were made on a large polycrystalline sample (diameter 8 mm) and a small single crystal (diameter 3.5 mm). The samples were grown by means of the Bridgeman technique. The starting material consisted of 25.2 at.% Al and 74.8 at.% Ni. This charge was put in an alumina crucible enclosed in a graphite tube, which was heated by RF currents. Both crucible and graphite tube were kept under a constant flow of pure argon (99.998%).

The homogeneity of the sample was improved by turning the ingot and remelting twice. The resulting rod was annealed for nine hours at 1350 °C under the same conditions. The samples used in the experiment were spark cut from this rod and then annealed at 1270 °C for two hours. To reduce possible carbon contamination of the sample they also were annealed under a wet hydrogen atmosphere at 1000 °C.

Laue photographs of the single crystal gave sharp reflections, indicating it to be a single crystal. The polycrystalline sample was also shown to be truly polycrystalline.

Finally the samples were polished using several powders, ending with 1 μm diamond powder. This resulted in perfectly shiny silver-like surfaces. Immediately after polishing, the samples were introduced into an ultra-high vacuum system and measurements were performed at a pressure of 10^{-9} Torr. In order to check the accuracy we performed the measurements on two different samples—a polycrystalline sample and a single crystal which came from the same melt and received identical treatment. The resulting measurements were in excellent agreement with each other, and we were able to reproduce the curves for ε_1, ε_2 and the optical conductivity to within 1%.

The large polycrystalline sample was sputtered for several hours at 10 μA cm^{-2} by 600 eV argon ions in order to remove possible oxide layers. This, even in the high-energy range, gave results which reproduced the other measurements to within 1%.

This is in agreement with expectations of an oxide layer of at most 50 Å, which is much less than the skin depth at the energies used (several hundred Å or more). For the single crystal the full energy range of our ellipsometer could not be used due to the resulting loss of light intensity after reflection from the small surface (10 mm^2). It could be measured up to 4.5 eV. The resulting dielectric constants are shown in figure 1.

The optical conductivity is given in figure 2 along with the calculated JDOS/ω. It clearly shows a large, broad peak centred at 4.32 eV. There is also a small shoulder which starts at 0.72 eV, ends at 1.10 eV and has a maximum at 0.86 eV; this shoulder is discernible in figure 2 and its position is marked with an arrow. In the experimental results as presented in figures 1 and 2 a Drude term, due to intraband transitions, is present and gives rise to a structureless background, which is large only in the infrared region. In order to check the Drude behaviour of Ni_3Al a plot of $\hbar\omega\varepsilon_2$ against $-\varepsilon_1$ (Argand diagram) was made. In the low-energy region before the onset of interband transitions the Argand diagram gives the following relation: $\hbar\omega\varepsilon_2(\omega)=(\hbar/\tau)(\delta\varepsilon_1^b-\varepsilon_1(\omega))$ where τ denotes the scattering time and $\delta\varepsilon_1^b$ is a constant contribution to ε_1 which, due to the Kramers–Kronig relations, arises from interband transition at high energies. This diagram yielded values of $\delta\varepsilon_1^b=20\pm4$ and $\tau=(1.0\pm0.5)\times10^{-15}$ s. A fit was made to ε_2 in the region 0.5–0.7 eV; assuming perfect Drude behaviour and the absence of interband transitions, this leads to $\omega_p=(13.5\pm0.5)\times10^{15}\ s^{-1}$ and $\tau=(3.4\pm0.3)\times10^{-16}$ s. Clearly the values are not in agreement, and the value found for τ by the latter method is very short. The deviations can be explained by the fact that interband transitions start at very low energies. This is

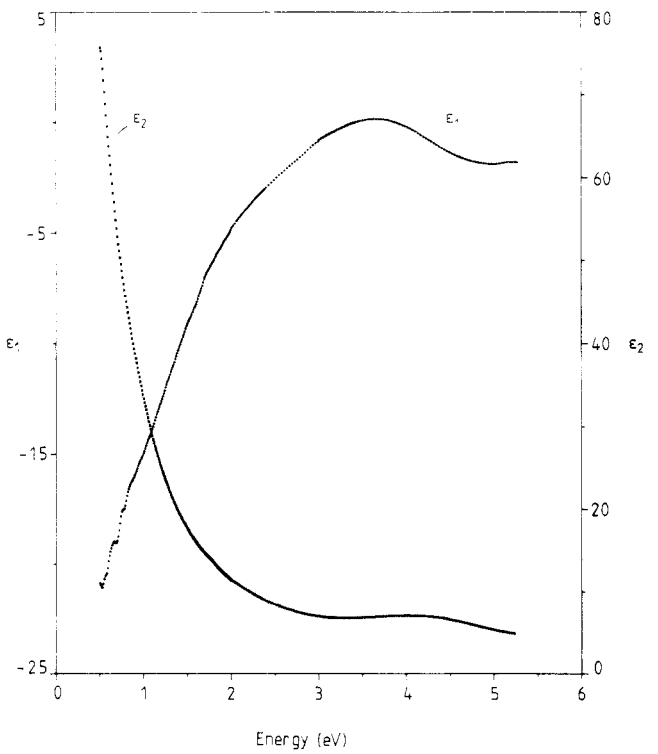

Figure 1. The real part of the dielectric constant ε_1 and the imaginary part of the dielectric constant ε_2 from the measured data.

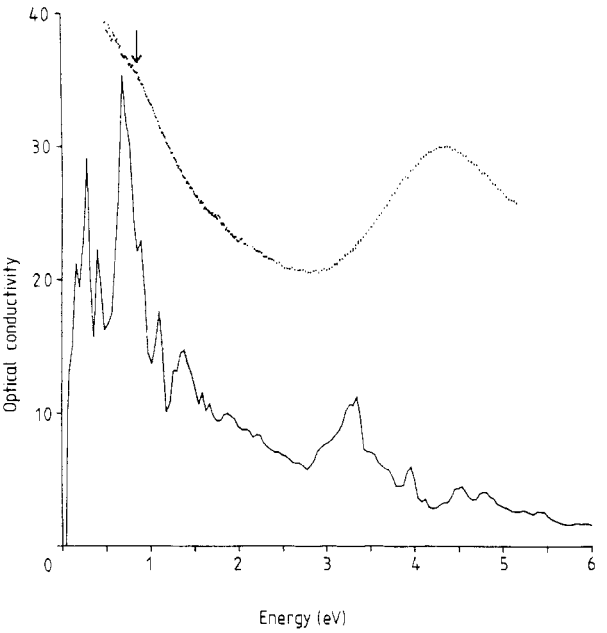

Figure 2. The optical conductivity of Ni_3Al from the experimental data (dots) and the JDOS/ω from the calculation (full curve, arbitrary units).

also the case for other d-band metals, e.g. nickel. It was not possible to separate the Drude and interband contributions further in the low-energy ranges.

3. Theory

The band structure along the high-symmetry lines is shown in figure 3. It is based on the self-consistent calculation of Buiting *et al* (1983). They used the ASW method of Williams *et al* (1979). The lattice constant used in the calculation (3.525 Å) was obtained by minimising the self-consistent total energy and is slightly smaller than the experimental value (3.568 Å). The energy-level diagram of figure 3 is the same in topology and connectivity as those presented by Hackenbracht and Kübler (1980) but deviates from the much simpler treatment of Fletcher (1972).

In figure 2 the combined results for the experimental optical conductivity and theoretical JDOS/ω are shown. The JDOS/ω resembles the optical conductivity when the matrix elements are considered to be constant. The theoretical JDOS/ω was calculated on basis of the band structure given in figure 3, using the same method as van der Heide *et al* (1984). The JDOS/ω was derived from the JDOS, which we obtained by integration over eight million pseudo-random points in the irreducible wedge ($\frac{1}{48}$th) of the simple cubic Brillouin zone. To make these large-scale calculations possible on a reasonable time scale we undertook the following steps. The lowest 22 bands, resulting from the ASW calculation were fitted to Fourier series containing 40 stars of reciprocal lattice vectors. The fit was made to 89 k-points in the irreducible wedge, obtaining a RMS error of about 1 mRyd. The fit was worst at points where bands cross and it could, in some cases, become as high as 10 mRyd.

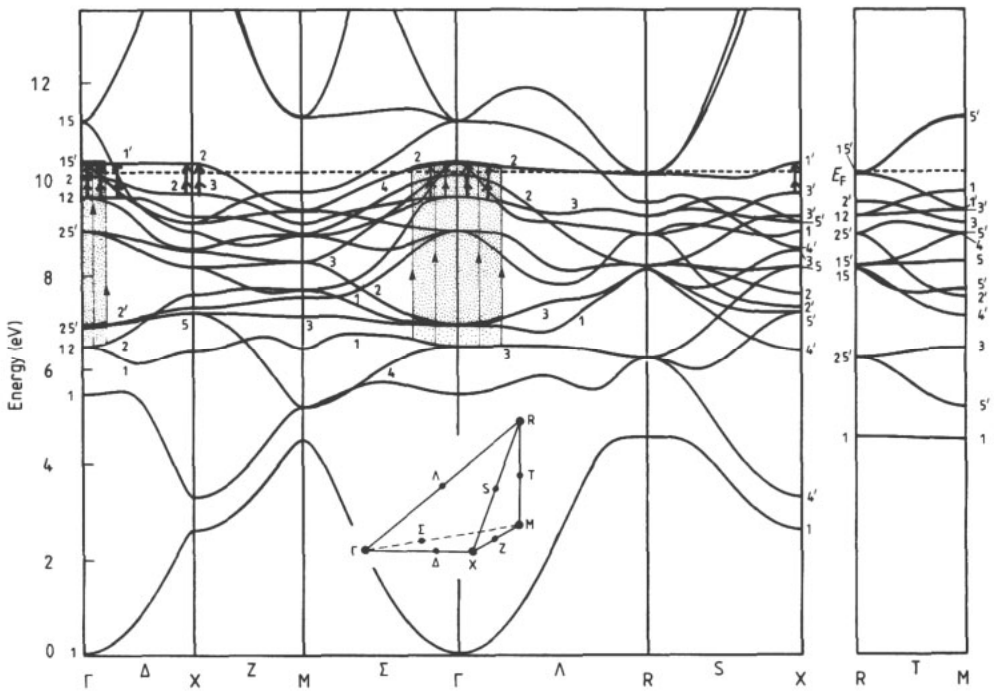

Figure 3. The band structure of Ni_3Al along the high-symmetry lines. The shaded areas indicate the transitions contributing to the peaks in the theoretical curve at 3.4 and 3.9 eV. The heavier shading indicates transitions from bands 5 and 6; the lighter shading refers to transitions from bands 3 and 4. The transitions contributing to the peak at 0.68 eV in the theoretical curve are indicated by arrows (↕).

Having obtained a good representation for the relevant energy bands in this way, the irreducible wedge was divided into 2000 small cubes and the eigenvalues at the corners of the cubes were calculated with the Fourier expansion. By using Lagrange interpolation we obtained the eigenvalues at 4000 random points inside each cube.

The essence of the calculation is then to make a histogram, sampling the quantity $E_n(\boldsymbol{k})-E_m(\boldsymbol{k})$ for all $n, m \in \{1, 2, \ldots, 22\}$ and all $\boldsymbol{k}$ in the $\frac{1}{48}$th of the Brillouin zone. The sampling was done with weight one, i.e. the elements of the transition matrix were considered to be constant.

The program also had the possibility of tracing which bands and $\boldsymbol{k}$-points contribute to a certain peak in the JDOS or JDOS/ω. The identifications we made in this way for certain peaks are indicated by the shaded areas and arrows in the energy-level diagram of figure 3.

4. Discussion

The experimental optical conductivity declines from 0.5 eV to a clear minimum at 2.80 eV. This first part of the optical conductivity contains a Drude contribution and a contribution from interband transitions. The shoulder at 0.86 eV in the experimental curve, indicated by an arrow in figure 2, possibly represents the peaks in the theoretical curve in this energy

region. The peaks represent transitions from bands 8, 9, 10, 11 and 12 to band 16 near Γ and from bands 15 and 16 to 17 near X, as indicated in figure 3.

The deviations from classical Drude behaviour can be explained by the fact that direct interband transitions for Ni_3Al start at very low energies, as predicted by the calculation.

The minimum at 2.80 eV is also present in the theoretical curve.

Between 2.8 and 5.3 eV we find a pronounced peak in the optical conductivity, which we identify as transitions between bands 5 and 6 (as well as 3 and 4) and bands 14, 15 and 16 in the neighbourhood of the point Γ. Transitions from bands 5 and 6 are indicated by the areas with heavy shading, and transitions from bands 3 and 4 by the areas with lighter shading.

The peak centred at 3.4 eV in the theoretical curve in figure 2 results from transitions from bands 5 and 6, while the theoretical peak at 3.9 eV results from transitions from bands 3 and 4. The final and initial states involved in these transitions have mainly nickel d character, although bands 3 and 4 also contain weak aluminium d states and are therefore comparable with the optical results for pure nickel as we will see later.

The shift between the experimental and theoretical peaks is roughly 0.7 eV. We assume that both peaks in the theoretical curve (at 3.4 and 3.9 eV) contribute to the broad experimental peak at 4.32 eV. The centre of gravity of the theoretical contribution would be at 3.6 eV. This would imply a shift of about 0.7 eV.

This shift can be partly explained by the fact that constant matrix elements were assumed in the calculation. This assumption influences peak heights severely and peak positions by a few tenths of 1 eV. Many-body effects may also influence the peak position.

The structure observed in the optical conductivity is due to transitions between states of mainly nickel character. It is therefore interesting to compare our results on Ni_3Al with earlier results on nickel (Ehrenreich *et al* 1963, Wang and Callaway 1974, Stoll and Jung 1979). In doing this we see a clear resemblance between the curves of the optical conductivity for Ni and Ni_3Al, which have qualitatively the same form. Nickel also shows a broad peak at 4.7 eV, although shifted 0.3 eV with respect to Ni_3Al. In the infrared range nickel shows two sharp peaks at 0.3 and 1.4 eV. In Ni_3Al there is also structure in this region, although not so pronounced as in Ni: Ni_3Al shows a small shoulder with a maximum at 0.86 eV.

Acknowledgments

Part of the research described was supported by the research program of the 'Stichting voor Fundamenteel Onderzoek der Materie' with financial support from the 'Nederlandse Organisatie voor Zuiver Wetenschappelijk Onderzoek'.

References

Beattie J R 1955 *Phil. Mag.* **46** 235
Bernhoeft N R, Lonzarich G G, Mitchell P W and Paul D McK 1983 *Phys. Rev.* B **28** 422
de Boer F R 1969 *Thesis* University of Amsterdam
Born M and Wolf E 1959 *Principles of Optics* (Oxford: Pergamon)
Buis N 1979 *Thesis* University of Amsterdam
Buiting J J M, Kübler J and Mueller F M 1983 *J. Phys. F: Met. Phys.* **13** L179
de Dood and de Châtel P F 1973 *J. Phys. F: Met. Phys.* **3** 1039
Ehrenreich H, Philipp H R and Olechna D J 1963 *Phys. Rev.* **131** 2469

Fletcher G C 1972 *Physica* **62** 41
Fuggle J C, Hillebrecht F U, Zeller R, Zolnierek Z, Bennett P A and Freiburg Ch 1983 *Phys. Rev.* B **27** 2145
Hackenbracht D and Kübler J 1980 *J. Phys. F: Met. Phys.* **10** 427
van der Heide P A M, Baelde W, de Groot R A, de Vroomen A R and Mattocks P G 1984 *J. Phys. F: Met. Phys.* **14** 1745
Lonzarich G G, Sigfusson T I, Buiting J J M, Kübler J and Mueller F M 1982 *J. Appl. Phys.* **53** 3
Stoll M P and Jung C 1979 *J. Phys. F: Met. Phys.* **9** 2491
Wang C S and Callaway J 1974 *Phys. Rev.* B **9** 4897
Williams A R, Kübler J and Gelatt C D Jr 1979 *Phys. Rev.* B **19** 1979